Carbohydrate Polymers 111 (2014) 797–805

Contents lists available at ScienceDirect

Carbohydrate Polymers

journal homepage: www.elsevier.com/locate/carbpol

Cationic hemicellulose-based hydrogels for arsenic and chromium removal from aqueous solutions

Daniel Dax[a,*], María Soledad Chávez[b,c], Chunlin Xu[a,d], Stefan Willför[a], Regis Teixeira Mendonça[b,e], Julio Sánchez[c,**]

[a] Process Chemistry Centre, c/o Laboratory of Wood and Paper Chemistry, Åbo Akademi University, Porthansgatan 3, 20500 Åbo/Turku, Finland
[b] Centro de Biotecnología, Universidad de Concepción, Casilla 160-C, Concepción, Chile
[c] Polymer Department, Faculty of Chemistry, University of Concepción, Casilla 160-C, Concepción, Chile
[d] Wallenberg Wood Science Center, KTH, The Royal Institute of Technology, 10044 Stockholm, Sweden
[e] Facultad de Ciencias Forestales, Universidad de Concepción, Casilla 160-C, Concepción, Chile

ARTICLE INFO

Article history:
Received 16 February 2014
Received in revised form 6 May 2014
Accepted 7 May 2014
Available online 27 May 2014

Keywords:
Crosslinking
Polysaccharide
O-Acetyl galactoglucomannan
Hemicellulose
Hydrogels
Wastewater treatment

ABSTRACT

In this work the synthesis of hemicellulose-based hydrogels and their application for the removal of arsenic and chromium ions is described. In a first step *O*-acetyl galactoglucomannan (GGM) was subjected to a transesterification applying glycidyl methacrylate (GMA) for the synthesis of novel GGM macromonomers. Two distinguished and purified GGM fractions with molar mass of 7.1 and 28 kDa were used as starting materials. The resulting GGM macromonomers (GGM-MA) contained well-defined amounts of methacrylate groups as determined by ^{1}H NMR spectroscopy. Selected GGM-MA derivatives were consecutively applied as a crosslinker in the synthesis of tailored hydrogels using [2-(methacryloyloxy)ethyl]trimethylammonium chloride (MeDMA) as monomer. The swelling rate of the hydrogels was determined and the coherence between the swelling rate and the hydrogel composition was examined. The morphology of the GGM-based hydrogels was analysed by SEM and the hydrogels revealed a high surface area and were assessed in respect to their ability to remove arsenate and chromate ions from aqueous solutions. The presented bio-based hydrogels are of high interest especially for the mining industries as a sustainable material for the treatment of their highly contaminated wastewaters.

1. Introduction

The rapid growth of the world population and the increasing living standard in developing countries leads to a constant augmentation of the need for construction materials, electronic components, and energy resources. Therefore, worldwide oil and coil, resp. ore deposits are exploited. Beside various other problems, one threatening side effect of the exploitation of ores is that the local environment is often highly contaminated with toxic heavy metals and metalloids such as mercury (Hg), chromium (Cr), arsenic (As), lead (Pb), cadmium (Cd), and zinc (Zn). Ions of these metallic species are found in the industrial wastewaters and they can be accumulated in the environment and tissues causing various diseases and disorders in living organisms. Because heavy metal ions show toxic effects even at very low dosages, an effective wastewater treatment is essential to avoid unnecessary exposure of the population in the surroundings of ore mines. Several methods for the removal of metal ions are known, such as the adsorption of metal ions on activated carbon (Faulconer, von Reitzenstein, & Mazyck, 2012), application of chelating or ion exchange resins (Zainol & Nicol, 2009), zeolites (Ali, Thabet, El-Nasser, Hassan, & Salama, 2012), as well as the use of synthetic polymers (Rivas, Pereira, Gallegos, & Geckeler, 2002; Rivas, Pereira, Palencia, & Sánchez, 2011) and chemical precipitations (Feng, Aldrich, & Tan, 2000). Nevertheless, these techniques have several inherent disadvantages such as high costs, formation of toxic sludge, and other waste products, which have to be disposed (Peng, Ren, et al. 2012; Peng, Zhong, et al. 2012). Extensive efforts are thus made in order to produce more efficient, environmentally friendly (e.g. biobased), and reusable materials for heavy metal removal from wastewaters. In the last decade, different plant materials such as lignin (Guo, Zhang, & Shan, 2008), cellulose (Akama & Ueda, 2013), chitin/chitosan (Ayoub, Venditti, Pawlak, Salam, & Hubbe, 2013; Zheng, Wang, Zhu, & Wang, 2013), hemicelluloses (Peng, Ren, et al. 2012; Peng, Zhong, et al.

* Corresponding author. Tel.: +358 2215 4886; fax: +358 2215 4868.
** Corresponding author. Tel.: +56 041 2207028; fax: +56 041 2245974.
E-mail addresses: ddax@abo.fi (D. Dax), juliosanchez@udec.cl (J. Sánchez).

http://dx.doi.org/10.1016/j.carbpol.2014.05.045
0144-8617/

2012), agriculture wastes (Ahluwalia & Goyal, 2005; Wan Ngah & Hanafiah, 2008), starch (Apopei, Dinu, Trochimczuk, & Dragan, 2012) and bark (Netzahuatl-Muñoz, Guillén-Jiménez, Chávez-Gómez, Villegas-Garrido, & Cristiani-Urbina, 2012; Palma, Freer, & Baeza, 2003) were tested in respect to their ability to absorb metal ions. From this list especially cellulose and hemicelluloses reveal a high potential due to their high abundance, as well as the already existing refining factories, e.g. pulp mills. Furthermore, the use of cellulose and hemicelluloses does not raise ethical issues because they cannot be used as food, what makes them favourable compared to starch.

One promising water-soluble hemicellulose is *O*-acetyl galactoglucomannan (GGM), which can be extracted from softwood by pressurized hot-water extraction (PHWE) (Al Manasrah, Kallioinen, Ilvesniemi, & Manttari, 2012) or recovered from the wastewaters of a thermomechanical pulping process by ultrafiltration (Lundqvist et al., 2003; Persson, Nordin, Zacchi, & Jónsson, 2007; Willför et al., 2003; Xu, Willför, Holmlund, & Holmbom, 2009). The circumstance that GGM is a side product of the pulping industry and hence available in large amounts, reveals the outstanding potential of GGM as a renewable raw material for novel functional products. GGM consists of a linear backbone of randomly distributed (1→4)-linked β-D-mannopyranosyl (Man*p*) and (1→4)-linked β-D-glucopyranosyl (Glc*p*) units, with α-D-galactopyranosyl (Gal*p*) units as single side units (Hannuksela & Hervé du Penhoat, 2004). GGM is partially acetylated and the *O*-acetyl groups are located randomly at C2 and C3 position of the mannose units in the main chain (Willför et al., 2003). In order to make GGM suitable for ion removal applications, water-soluble GGM derivatives bearing different, either charged or neutral, groups might be synthesized. The most convenient way to modify GGM is the substitution of the hydroxyl groups (Dax, Eklund, et al., 2013; Dax, Xu, et al., 2013; Voepel, Edlund, Albertsson, & Percec, 2011), but charged polymers can also be attached to the reducing end of GGM (Dax, Eklund, et al., 2013; Dax, Xu, et al., 2013). These GGM derivatives would be water-soluble and could be applied for metal removal in a similar way as water-soluble synthetic polymers. However, the complex setup needed when using water-soluble polymers makes it preferable to develop water-resistant products, such as hydrogels based on bio-renewable materials. These materials could be removed from the aqueous solution either by filtration or centrifugation, which makes the use of, e.g. expensive special membranes superfluous.

In this work, an effective way for the synthesis of novel, tailor-made GGM-based hydrogels with tuneable swelling rates is described. Two purified and well-characterized GGM fractions were in a first reaction step derivatized in a transesterification reaction with glycidyl methacrylate and analysed by ^{1}H and ^{13}C NMR. Subsequently, the GGM macromonomers were applied as bio-based crosslinkers in the production of several hydrogels using a methacrylic monomer bearing a quaternary ammonium group. The GGM-based hydrogels were tested with respect to their potential as a bioadsorbent by removing toxic As and Cr ions from aqueous solutions.

2. Experimental

2.1. Materials

Glycidyl methacrylate (GMA) 97% (Aldrich), ammonium persulfate 98% (Aldrich), [2-(methacryloyloxy)ethyl] trimethylammonium chloride (MeDMA) 80 wt.% in H_2O (Aldrich), dimethyl sulfoxide (DMSO) (Merck), dimethylformamide (DMF) (Aldrich), acetone (J.T. Baker), 4-(dimethylamino)pyridine (DMAP) 98% (Aldrich), ethanol (EtOH) (Merck), $Na_2HAsO_4{\cdot}7H_2O$ (Merck), $K_2Cr_2O_7$ (Merck), NaOH (Merck), HNO_3 (Merck). DMSO and DMF were distilled to remove water. All the other materials were commercially available and were of reagent grade or better and were used without further purification.

Table 1
Reaction conditions for the transesterification of GMA with GGM.

Crosslinker	*T* (°C)	GMA/X[a]	DMAP[b]	Solvent	MA per GGM chain[c]	DS_{MA}
GGM5-MA0.04	50	5:7	5	DMF	0.97	0.03
GGM5-MA0.25	50	5:7	10	DMF	6.89	0.25
GGM5-MA0.32	50	5:7	20	DMF	8.87	0.32
GGM5-MA0.03	50	5:7	10	DMSO	0.87	0.03
GGM5-MA0.14	50	5:7	20	DMSO	3.78	0.14
GGM5-MA0.33	50	10:7	20	DMSO	9.23	0.33
GGM22-MA0.41	50	5:7	20	DMF	50.78	0.41
GGM22-MA0.32	50	5:7	20	DMSO	39.7	0.32
GGM22-MA0.20	50	2.5:7	20	DMSO	24.7	0.20

[a] Molar ratio of GMA to anhydrous sugar units of GGM.
[b] wt.% in respect to GGM.
[c] Average amount of MA groups present in each GGM chain.

Pressurized hot-water extracted *O*-acetyl galactoglucomannan (GGM) from Norway spruce (*Picea abies*) was provided by The Finnish Forest Research Institute Metla. The extraction conditions were studied and optimized in a previous study (Kilpeläinen, Kitunen, Pranovich, Ilvesmiemi, & Willför, 2013) and GGM was obtained as a solution with a concentration of 30 wt.%. The extract was further purified in order to remove impurities and to narrow down the molar mass distribution (low polydispersity (PDI)). Therefore, the concentrated GGM solution (330 mL) was diluted with water (670 mL) and then precipitated in 9 L of ethanol at room temperature. The colourless precipitate was filtrated off and consecutively washed with ethanol, acetone, and methyl *tert*-butyl ether and finally the solid GGM was freeze-dried. The purified GGM fraction was obtained with a weight average molar mass (M_w) 7.1 kDa (polydispersity ~ 1.5). The second GGM fraction was prepared from the process water of spruce thermomechanical pulping (TMP) prior to any chemical treatments (Willför et al., 2003). In short, the process water was purified from colloidal wood resin, and aromatic residues using a cationic coagulant (Raifix 120, Raisio Chemicals Oy, Finland) and XAD-7 resin (Amberlite, Rohm and Haas, UK). The solution was concentrated under reduced pressure before GGM collected by precipitation in ethanol. The GGM was air-dried and its M_w was 28 kDa (polydispersity ~ 1.3), as determined by HPSEC-RI/MALLS. In the following text the GGM fractions are referred as GGM5 (M_n = 4.7 kDa) and GGM22 (M_n = 21.5 kDa). The sugar unit ratio of GGM was determined by acid methanolysis and gas chromatography and was around 5–4:1:0.5–1.1(Man:Glc:Gal) (Willför, Sundberg, Tenkanen, & Holmbom, 2008) and the degree of acetylation (DS_{Ac}) ~ 0.20.

2.2. Synthesis of GGM-MA macromonomers

The reaction conditions for the insertion of the methacrylate groups into the GGM chain were adjusted outgoing from a previous study (Peng, Ren, et al. 2012; Peng, Zhong, et al. 2012) by changing the temperature, the catalyst amounts, and the solvent. The parameters of the performed reactions are listed in Table 1. The exact procedure is exemplarily described for the product GGM5-MA0.03 (here 0.03 denotes the degree of substitution of GGM5). GGM5 (100 mg, 0.6 mmol of anhydrous sugar units, 1 equiv.) was dissolved in 3 mL of dry DMF at 50 °C. Consecutively DMAP (5 mg, 0.041 mmol, 5 wt.% in respect to GGM) and GMA (62 mg, 0.43 mmol, 0.7 equiv.) were added and the mixture was stirred under nitrogen atmosphere at 50 °C for 16 h. The reaction mixture was then transferred into a dialyses tube (cut-off of 2 kDa) and dialyzed against distilled water for 3 days with daily water

exchange. The aqueous solution of the product was dried by consecutive evaporation under reduced pressure and storage in the oven at 50 °C overnight. A brownish solid was obtained (62.7 mg, yield 62%). ^{1}H NMR (600 MHz, D_2O, 25 °C, ppm): δ 1.81–2.00 (s, 3 H, CH_2=C–CH_3), 2.04–2.22 (m, 3 H, –CO–CH_3), 3.09–5.56 (non-anomeric and anomeric protons of GGM, more details in Fig. 2), 5.70–5.87 (m, 1 H, C=CH_2), 6.09–6.33 (m, 1 H, C=CH_2); ^{13}C NMR (600 MHz, D_2O, 25 °C, ppm): 17.47 (CH_2), 20.27 (–CO–CH_3), 59.75–77.48 (non-anomeric GGM carbon signals, details in Fig. 3), 98.41–103.3 (anomeric GGM carbon signals), 127.47 (CH_2=C–CH_3).

2.3. Synthesis of the GGM-based hydrogels

Exemplary the synthesis of [GGM5-MA0.14;20;10;5] is described. The products of the polymerization were labelled as follows: [(GGM-MA derivative used); (wt.% of GGM-MA + monomer in the reaction solution); (wt.% of GGM-MA in respect to the monomer); (mol% of the initiator in respect to the monomer)]. GGM5-MA0.14 (50.0 mg, 0.01 mmol), MeDMA (450 mg, 2.16 mmol) and ammonium persulfate (24.7 mg, 0.11 mmol) were dissolved in 2.0 mL of de-ionized water and N_2-gas was bubbled into the solution for 15 min in order to remove oxygen. Subsequently the reaction tube was placed in an oil bath at 75 °C for 2 h. After the reaction was completed, the formed hydrogel was placed in 200 mL of de-ionized water in order to remove unreacted monomers and loose polymer chains from the hydrogel. After drying in the oven at 40 °C, a pure GGM-based hydrogel was obtained.

2.4. Swelling

The swelling ratio was determined by placing 100–200 mg of the dried GGM-based hydrogel in 200 mL of de-ionized water. After 24 h at room temperature, the hydrogel was removed from the solution. Water that remained on the surface of the hydrogel was carefully removed using a paper filter. The weight of the swollen hydrogels was determined and the swelling ratio (Q) was calculated using Eq. (1):

$$Q = \frac{m_t - m_0}{m_0} \quad (1)$$

where m_t is the weight of the hydrogel at the time t and m_0 is the initial weight of the oven dried sample (Albertsson, Voepel, Edlund, Dahlman, & Söderqvist-Lindblad, 2010; Zheng et al., 2013).

2.5. High performance size exclusion chromatography (HPSEC)

The weight- and number-average molar mass (M_w and M_n) and molar mass distribution (MWD) of native GGM were determined by HPSEC in on-line combination with a multi-angle laser light scattering (MALLS) detector (miniDAWN, Wyatt Technology, Santa Barbara, USA) and a refractive index (RI) detector (Shimadzu Corporation, Japan). A two-column system, 2× UltrahydrogelTM linear 300 mm × 7.8 mm column (Waters, Milford, USA), in series was used. 0.1 M $NaNO_3$ was used as the elution solvent. The flow rate was 0.5 mL min^{-1}. A dn/dc value of 0.150 mL g^{-1} was used (Michielsen, Brandrup, & Immergut, 1999). The samples were filtered through a 0.22 μm nylon syringe filter before injection. The injection volume was 100 μL. Astra software (Wyatt Technology, Santa Barbara, USA) was used to analyse the data.

2.6. Nuclear magnetic resonance spectroscopy (NMR)

The native GGM and the GGM-MA derivatives were analysed by ^{1}H and ^{13}C NMR measurements using a Bruker Avance spectrometer (operation frequency: ^{1}H: 600.13 MHz; ^{13}C: 150.92 MHz). Either D_2O or DMSO-d_6 was used as solvent and the temperature for all the experiments was set to 25 °C. For the ^{1}H NMR spectra 50 scans were made and for the ^{13}C NMR 20000 scans were required to assure a good resolution.

2.7. Determination of the degree of acetylation and calculation of the degree of substitution

The degree of acetylation (DS_{Ac}) for the native GGM was determined by titration following a procedure described earlier (Xu et al., 2010). The DS_{Ac} obtained by titration was used as reference and the DS_{Ac} for all the GGM derivatives was determined by evaluating the respective ^{1}H NMR spectra.

The degree of substitution (DS_{MA}) of the GGM derivatives was determined by ^{1}H NMR measurements. Therefore the ^{1}H NMR spectra were calibrated using a method described earlier (Dax, Eklund, et al., 2013; Dax, Xu, et al., 2013) (detailed procedure can be found in the supporting information). For GGM5 the peak region from 3.2 to 4.4 ppm was set to 162.5 and for GGM22 to 727.9. Because the number average molar mass was used for the calculations, the integration of the peak area from 1.81 to 2.06 ppm will directly give information about the amount of MA groups present in one GGM chain. The DS_{MA} value can hereafter be calculated using Eq. (2):

$$DS_{MA} = \frac{I_{CH_3}}{3 \times n_s} \quad (2)$$

where I_{CH_3} is the integration value of the CH_3 group of the inserted MA group (corresponds to three protons) and n_s is the number of anhydro-sugar units present in the GGM chain (the calculations of n_s can be found in the supporting information).

2.8. Fourier transformed infrared spectroscopy (FTIR)

The infrared spectroscopy measurements were performed with a Bruker ALPHA series using the ALPHA platinum ATR single reflection diamond ATR module. The samples were directly placed on the ATR plate for the measurements. The results were evaluated using the software OPUS from Bruker.

2.9. Scanning electron microscopy (SEM)

Before the SEM measurements, the samples were fully swollen in de-ionized water and consecutively freeze-dried. The SEM images were recorded using a Cameca model SU-30 SEM Probe in order to analyse the morphology of the hydrogel. The acceleration voltage for the measurement was 10 kV.

2.10. Toxic ion removal from aqueous solutions

To determine the arsenic and chromium sorption capacity of the hydrogels, a batch procedure was applied for the prepared and grinded hydrogels in separate experiments. All experiments were performed in a flask mounted on a shaker. Sorption equilibrium experiments were carried out in order to study the effects of the swelling rate of the hydrogels and the pH value of the solutions. Furthermore, successive batch experiments using the same hydrogel sample were performed to estimate the maximum sorption capacities of the hydrogels. The sorption capacity (S) of the hydrogel is determined by Eq. (3):

$$S = \frac{(C_i - C_f)V}{m} \quad (3)$$

where S is the amount of As(V) or Cr(VI) sorbed into the hydrogel matrix (mg metal sorbed per g of hydrogel). C_i and C_f (mg/L) are the concentrations of the ions in the solution before and after the

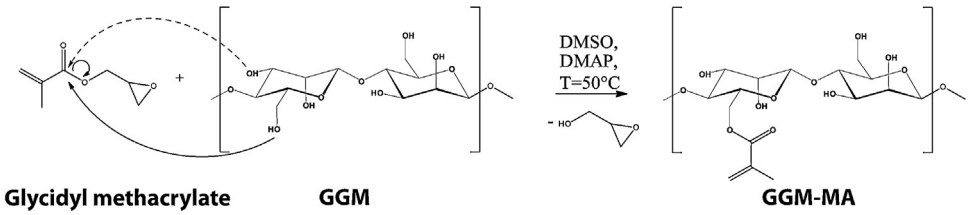

Fig. 1. Transesterification of GGM by glycidyl methacrylate using DMAP as a catalyst and DMSO as a solvent.

sorption by the hydrogels. *V* is the volume (L) of the aqueous phase and *m* is the mass of the dried hydrogel (g).

For the sorption experiments, 20 mg of dried hydrogel were added to 10 mL of As(V) or Cr(VI) ions solutions and consecutively shaken for 24 h at 25 °C. The initial concentration of the As(V) resp. Cr(VI) ions was 100 mg/L and the pH value was adjusted using 0.1 M NaOH and HNO_3. After the sorption, the hydrogel samples were filtered off and washed with water having the same pH value as the initial ion solution. The metal ion concentrations in the filtrates were determined by atomic adsorption spectroscopy (AAS) (Unicam Solaar 5M series). For the AAS a flame atomizer with 40% acetylene and 60% oxygen was used and an electrode discharge lamp (EDL) was used as a radiation source. The detected wavelengths were 193.7 nm for arsenic and 357.9 nm for chromium.

3. Result and discussion

3.1. Synthesis of GGM-MA crosslinker

The GGM-MA crosslinker was synthesized using GMA as methacrylate source and DMAP as a catalyst. The transesterification conditions were optimized for the GGM5 and GGM22 (7.1 kDa and 28 kDa, respectively) in order to generate GGM-MA derivatives with a desired degree of substitution of methacrylate groups (DS_{MA}). The reaction pathway is shown schematically in Fig. 1 and it was assumed that all hydroxyl groups of GGM can be converted.

The temperature was set to 50 °C to assure a high reaction rate and dry DMSO or DMF were used as solvents. The reaction mixtures were kept under N_2 atmosphere and the reaction parameters for some selected reactions are listed in Table 1. It was found that when DMF was used as a solvent, a higher DS_{MA} could be reached compared to DMSO for equal reaction conditions. It can be assumed that the better solubility of the MA-derivatized GGM in DMF led to a higher reaction velocity compared to DMSO. Furthermore, the use of higher amounts of catalyst leads to a higher conversion of the GMA. It was found that the higher the GMA content in the reaction mixture was, the higher were the DS_{MA} values determined by ^{1}H NMR. It has to be noted that even though DMF leads to slightly higher conversions of GMA, DMSO is preferred as a solvent due to its non-toxicity and because GGM22 showed, because of its high molar mass, low solubility in DMF.

The GGM5-MA and GGM22-MA derivatives were all readily soluble in water and were analysed by ^{1}H and ^{13}C NMR using D_2O as a solvent in order to define the exact DS_{MA} values. The assignment of the signals in the proton spectra of GGM5 and GGM5-MA0.33 are exemplary shown in Fig. 2. The anomeric protons (H-1 and H-1″) of the sugar units, as well as the protons at the carbon next to the acetyl-groups (H-9) gave signals in the peak region from 4.42 to 5.62 ppm. The signals of the other sugar protons from GGM (H-(2–6)) are situated in the peak region from 3.08 to 4.42 ppm. The CH_3 protons of acetyl groups gave signals from 2.07 to 2.26 ppm. In the spectrum of the GGM5-MA0.33, three additional peak areas could be identified. The CH_3 groups (H-11) of the methacrylate attached to GGM gave signals from 1.81 to 2.06 ppm. The two protons on the unsaturated carbon (H-12) gave signals in the regions 5.70–5.91 and 6.09–6.38 ppm. The DS_{MA} for the different GGM-MA derivatives was determined using the integration value of the peak area from 1.81 to 2.06 ppm as a reference. The DEPT-135 spectrum of the GGM-MA crosslinker confirmed the successful conversion of GMA in the presence of DMAP (Fig. 3). The signals of the native GGM chain are divided in two peak regions from 59.75 to 77.48 ppm (C-(2–6), 9, 10) and from 98.41 to 103.03 ppm (C-1 and C-1″). Furthermore the signal of the CH_3 carbon (C-7) of the acetyl-groups could be separately detected at 20.27 ppm. In the spectrum of the GGM-MA crosslinker the signal at 17.46 ppm could be assigned to the CH_3 group (C-11) of the methacrylate and the unsaturated carbon (C-12) of the methacrylate was detected at 127.47 ppm. The FTIR spectra for native GGM and the GGM-MA derivatives were recorded at room temperature (Fig. S1 in the supporting information). The carbonyl signal at 1722 cm^{-1} is stronger in the

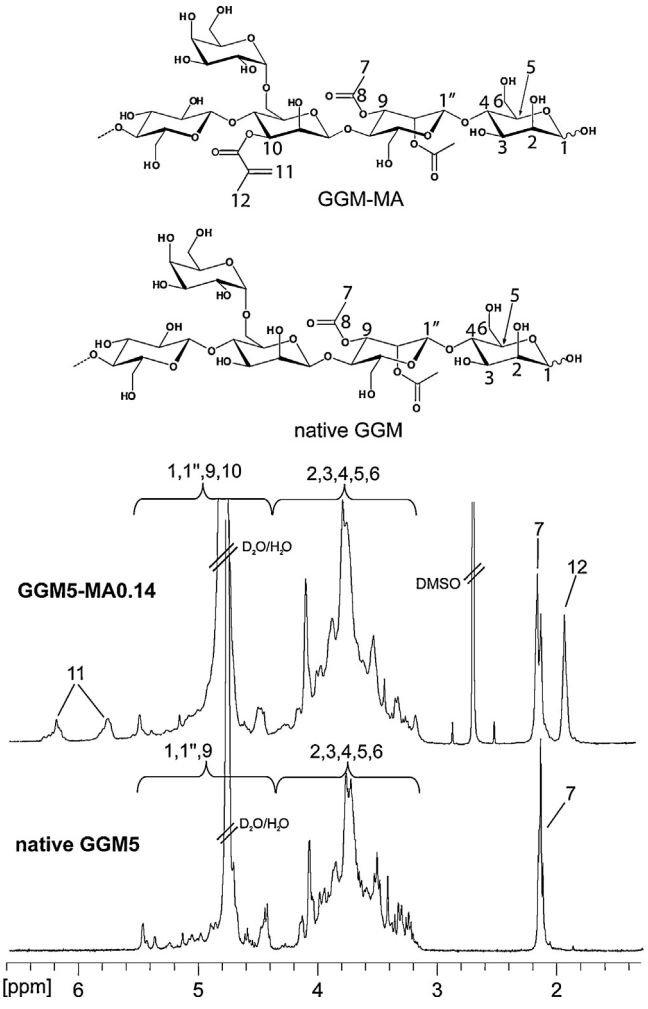

Fig. 2. ^{1}H NMR spectra of native GGM (GGM5) and a GGM5-MA crosslinker (GGM5-MA0.14) in D_2O.

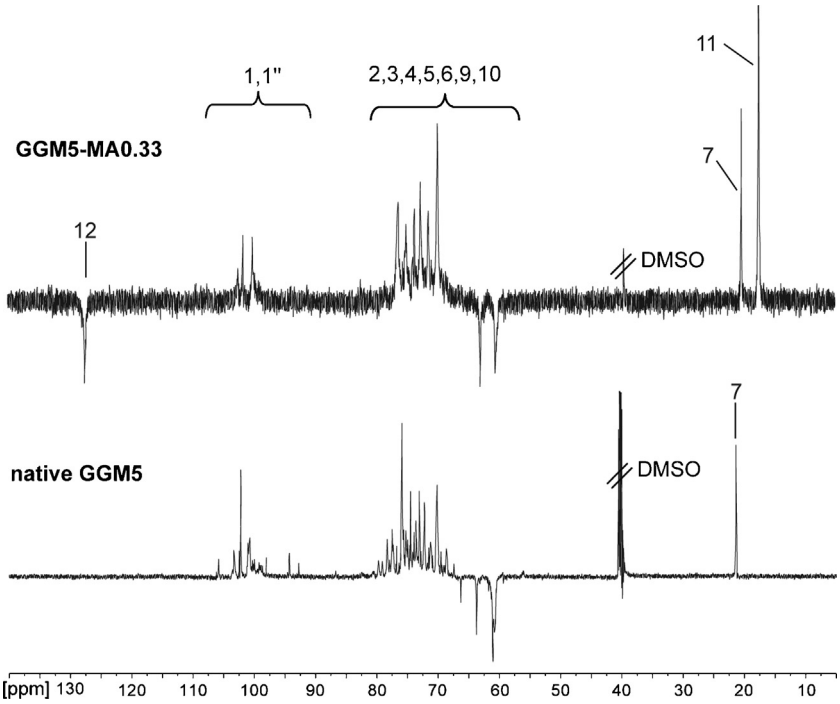

Fig. 3. DEPT-135 spectra of native GGM5 and a GGM5-MA crosslinker (GGM-MA0.33) recorded in DMSO-d_6 and D_2O, respectively.

GGM-MA derivative compared to the native GGM signal due to the introduced methacrylate groups. Also the CH_2 resp. CH_3 signals in the wavenumber range from 2875 to 2969 cm^{-1} corresponding to the C—H stretch vibration are stronger for the GGM-MA derivatives arising from the supplementary CH_3 groups from the methacrylate groups. The amplification of the signal at 1657 cm^{-1} in the GGM-MA derivatives was assigned to the C=C stretch of the unsaturated carbon atoms. Furthermore the peaks at 1311 and 808 cm^{-1} could be assigned to the C—H bending signals of the introduced functional groups.

3.2. Synthesis of GGM-based hydrogels

Several GGM-based hydrogels were synthesized using the different GGM-MA derivatives, varying amounts of monomer, as well as different amounts of initiator. For all the hydrogels, a GGM-MA derivative was dissolved in de-ionized water followed by the addition of the monomer and the initiator. Subsequently, nitrogen gas was bubbled into the reaction solution in order to remove the oxygen. Hereafter, the reaction flask was closed and heated up to 75 °C using an oil bath. A considerable increase in the viscosity could already be observed after 5 min and after 2 more hours at 75 °C, the resulting hydrogels were swollen in an excess of de-ionized water to remove all the molecules which were not linked to the hydrogel network. The hydrogels were oven-dried and the swelling rate (Q) was defined (Table 2). It was found that the swelling rate followed a logical trend in respect to the hydrogel composition.

Table 2
Swelling rate (Q) for different GGM-based hydrogels.

Hydrogel composition	Q
[GGM5-MA0.14;10;10;5]	57.6
[GGM5-MA0.14;20;10;5]	68.6
[GGM22-MA0.20;20;7;1]	26.6
[GGM22-MA0.20;20;10;5]	18.4
[GGM22-MA0.32;20;10;5]	6.6

For the hydrogels [GGM5-MA0.14;20;10;5] and [GGM22-MA0.20;20;10;5], low M_w resp. high M_w GGM-MA derivatives were used for which the DS_{MA} was comparable. All the other parameters during the hydrogel synthesis were the same (same amount of initiator and monomer) and it could be observed, that for the GGM5-MA derivative the swelling rate was 3.7 times higher than for the GGM22-MA derivative. Because the GGM22-MA contains more than six times more MA groups per molecule, denser networks are formed compared to the GGM5-MA with a similar DS_{MA}. In Scheme 1 this circumstance is visualized for the simplified case if there would only be one radical and hence only one polymer chain growing in the reaction solution.

Firstly, the polymer chain will attach to one GGM-MA (N°1) and consecutively continue growing and attach to a second GGM-MA. The active polymer chain end can then react with a third GGM-MA (N°2). Up to this moment the three chains are still flexible (for GGM5-MA, as well as for GGM22-MA) and could during swelling delocalize from each other to a maximum extent only restricted by the length of the two interlinking synthetic polymer chains. The crucial moment with respect to the swelling potential of the material occurs when the three GGM-MAs are merged another time (N°3). Now the GGM-MA chains of the interlinked network cannot depart from each other anymore and the swelling capability of the hydrogel is dramatically reduced. The reduced swelling of the hydrogels using GGM22-MA as a crosslinker compared to GGM5-MA is due to the higher probability of the formation of these crosslinked networks containing a minimum of three GGM-MA's (highlighted in red, N°4). When using the GGM22-MA with a DS_{MA} of either 0.20 or 0.32 for the hydrogel synthesis with equal amounts of initiator and monomer ([GGM22-MA0.20;20;10;5] and [GGM22-MA0.32;20;10;5]), the swelling rate for the GGM-MA0.32 based hydrogel was 2.7 times lower than for the GGM22-MA0.20 one. This is logical, because GGM22-MA0.32 contains more MA groups and hence is the more efficient crosslinker. This leads to a denser network formation with shorter polymer chains and hence to a reduced swelling potential. One hydrogel with a smaller amount of GGM-MA and smaller

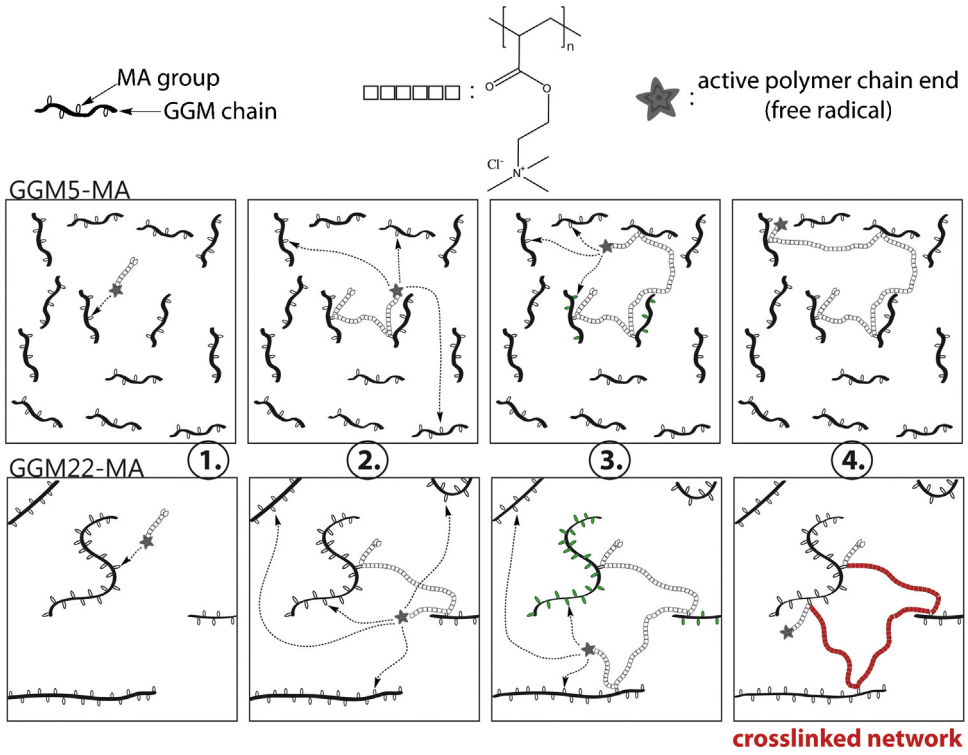

Scheme 1. Simplified illustration of the effect of the molar mass of the GGM-MA crosslinkers. 1 and 2: the active polymer chain reacts consecutively with three GGM-MA chains; 3: higher probability for interlinking of the three GGM22-MA chains compared to GGM5-MA because of the higher amount of MA groups (highlighted in green); 4: crosslinked network (for GGM22-MA).

amount of initiator was produced ([GGM22-MA0.20;20;7;1]) and it could be observed that the swelling rate was increasing compared to [GGM22-MA0.20;20;10;5] due to the smaller amount of radicals in the solution. This leads to the formation of longer polymer chains, which in combination with a lower amount of crosslinking points, resulting in a less dense network.

In Fig. 4, a series of photographs of [GGM5-MA0.14;20;10;5] illustrate the swelling of the GGM-based hydrogels. At $t = 0$ the hydrogel was water-free after oven drying and showed a brownish colour, which likely aroused from the synthetic polymer. After merging the solid hydrogel into a large excess of water, it started swelling and it could be observed that after 10 min the brown colour vanished in the outer area of the sample. After 120 min the hydrogel had taken up around 15 times the amount of water with respect to its initial weight. It could also be seen that up to that moment the physical consistency of the hydrogel was stable and only a light yellow stain was left in the core of the structure. After 22 h the hydrogel was fully swollen ($Q = 68.6$) and broke into smaller fragments. The fully swollen hydrogel was completely transparent.

3.3. Characterization of the morphology of the GGM-based hydrogels

Fig. 5 illustrates typical SEM images of a fully swollen and consecutively freeze-dried GGM-based hydrogel ([GGM5-MA0.14;10;10;5]). The low-magnification image (Fig. 5(a)) displays an overview of the sample and it could be observed that the hydrogel is present as unevenly shaped particles with a smooth surface. It has to be assumed that this surface morphology of the individual particles was formed during the freeze-drying process. Notably, after the drying process the cross-sectional area of broken particles reveals a highly porous structure (Fig. 5(b)). The high amplification image (Fig. 5(c)) features the extended surface of the material and led to the assumption that most of the quaternary ammonium groups are accessible for ion exchange in the swollen hydrogel.

3.4. Sorption of As(V) and Cr(VI) as a function of the swelling rate

In order to estimate the potential of the GGM-based hydrogels for treatment of wastewater, different sorption experiments were carried out. The sorption of As(V) and Cr(VI) was studied by applying different hydrogels with distinguished swelling rates (detailed in Table 2) in sorption experiments. The experiments were performed at pH 9 to ensure that the ions of arsenic and chromium were present in anionic form. In Fig. 6, the sorption (S) as a function of the swelling rate (Q) is shown. For As(V), a higher sorption was determined for an increasing swelling rate. This is due to the increased amount of quaternary ammonium groups of the material available for ion exchange with arsenic oxy-anions due to the increased surface area inside the hydrogel. The maximum sorption corresponds to 48.17 mg As(V) sorbed per g of hydrogel (sample [GGM5-MA0.14;20;10;5]). The sorption capacities were considerably higher compared to commercial resins such as Amberlite IRA 400-Cl, which revealed a maximum sorption at identical conditions of 27.1 mg/g (Rivas & Muñoz, 2009) (details about the resin can be found in the supporting information). The chromate ion sorption was higher than for the arsenic ions for low swelling rate and reached a maximum for the hydrogel [GGM22-MA0.20;20;7;1]. In general, hydrogels showed efficient sorption capacities for arsenates and chromates with the tendency of being more efficient the higher the swelling rate.

3.5. Effect of pH on the sorption of As(V) and Cr(VI)

In order to estimate in which pH range the GGM-based hydrogels show the highest performances, sorption experiments at three different pH values were carried out using

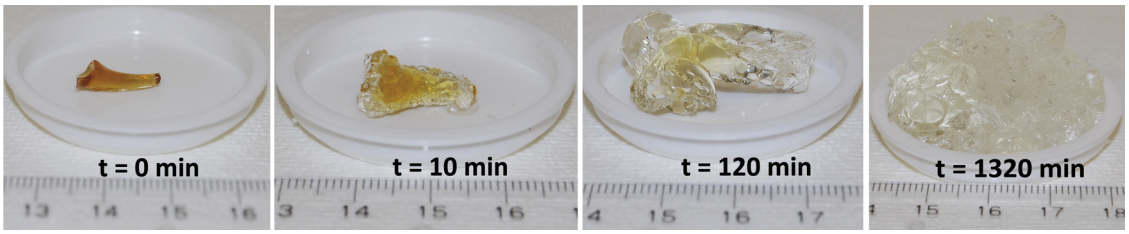

Fig. 4. Swelling behaviour of [GGM5-MA0.14;20;10;5]; 0.150 g of the dried hydrogel was able to take up 10.4 mL of water.

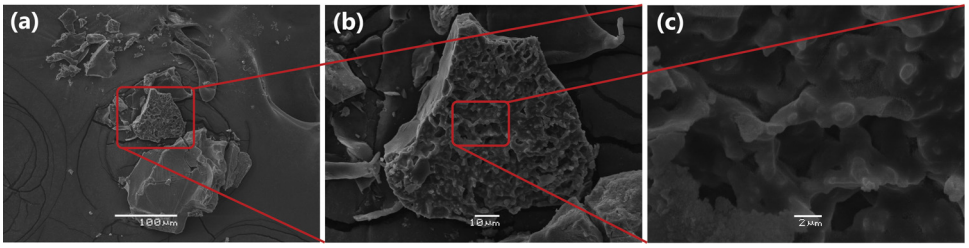

Fig. 5. SEM images of a fully swollen GGM-based hydrogel ([GGM5-MA0.14;10;10;5]) after freeze-drying.

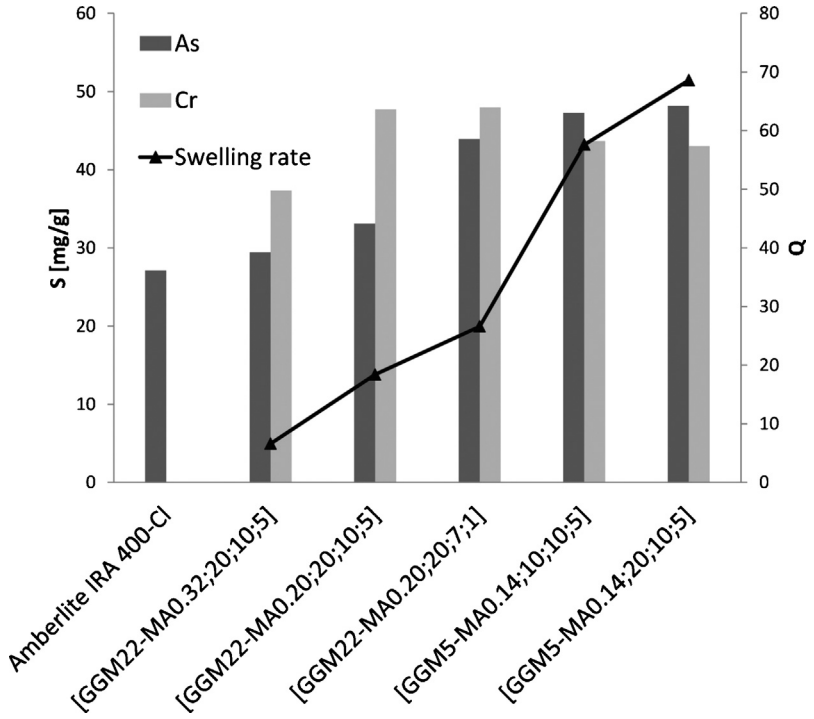

Fig. 6. Sorption of As(V) and Cr(VI) for different hydrogels and Amberlite IRA 400-Cl as a commercial product.

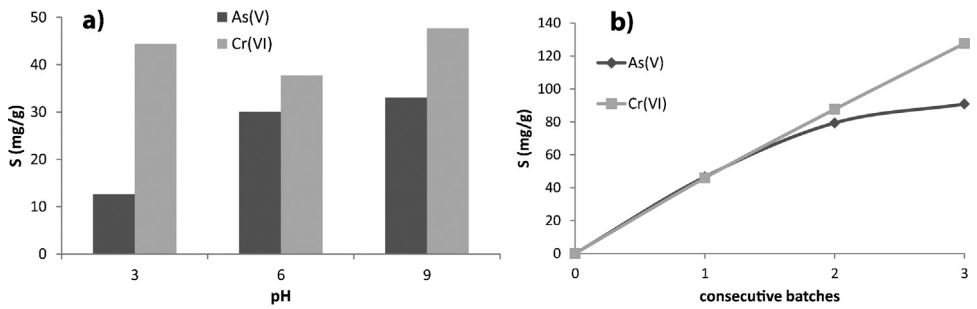

Fig. 7. (a) Sorption of As(V) and Cr(VI) in function of pH for the hydrogel [GGM22-MA0.20;20;10;5]; (b) sorption of As(V) and Cr(VI) in function of successive batches using [GGM22-MA0.20;20;7;1].

[GGM22-MA0.20;20;10;5]. Arsenate revealed higher sorption at pH 6 and at pH 9 in comparison with pH 3. At pH 3, mostly the monovalent anionic specie ($H_2AsO_4^-$) (Fig. S2 in the supporting information) is present and it is assumed that its lower charge density compared to $HAsO_4^{2-}$ lead to a reduced ion exchange. At pH 6, the monovalent ($H_2AsO_4^-$) and divalent ($HAsO_4^{2-}$) oxy-arsenic species exist in equilibrium (Sánchez, Bastrzyk, Rivas, Bryjak, & Kabay, 2013) and the sorption increased compared to pH 3. The higher retention of As by the hydrogel at pH 9 can be attributed to the divalent species (see Fig. 7a). In the case of chromate, the highest retention capacity was reached at pH 9, where divalent anionic CrO_4^{2-} species are predominant. The chromium removal was lower at pH 6 because CrO_4^{2-} and $HCrO_4^-$ ions exist in equilibrium. At pH 3, the sorption was similar to that at pH 9 due to the presence of $Cr_2O_7^{2-}$ ions. The sorption of chromate by the GGM-based hydrogel was high at a wide pH range, which could facilitate the application of the hydrogel for wastewater treatment.

3.6. Sorption capacity of As(V) and Cr(VI) in successive batches

The study of the maximum sorption capacity of the hydrogel was carried out with [GGM22-MA0.20;20;7;1] in successive batches using the conditions described in the experimental part. The results are shown in Fig. 7b and after the first batch, a similar S value for As(V) and Cr(VI) (around 40 mg/g) was determined. After that, the loaded hydrogel was submitted to a second batch (solution 100 mg/L of As(V) resp. Cr(VI)). The results showed that the hydrogel could remove similar amounts of ions as for the first batch reaching values around 80 mg/g. In a consecutively performed third batch, it could be observed that the hydrogel still removed the chromate ions in a constant rate compared to the two first batches reaching a maximum value of $S = 127$ mg/g. However, in the case of the arsenic ions a reduced up-take capacity for the third batch was assessed, indicating saturation of the active groups in the hydrogels.

4. Conclusions

Two GGM fractions (M_w of 7.1 and 28 kDa) were successfully modified by GMA in a transesterification reaction in the presence of DMAP. DMSO and DMF were tested as solvents for the modification of GGM and it was found that the use of DMF lead to slightly higher conversions compared to DMSO. Several GGM-MA derivatives were synthesized and the DS_{MA} determined by ^1H NMR was between 0.03 and 0.41. A selection of GGM-MA products was applied as crosslinker in the formation of bio-based hydrogels using a monomer bearing a quaternary ammonium group. The swelling rate for the different hydrogels was determined and a correlation between the DS_{MA} and the nature of the GGM chain could be assessed. The higher the GGM molar mass and the higher the DS_{MA} was, the higher the determined swelling rate was due to the formation of denser networks. Five distinguished hydrogels were tested with respect to their ability to remove Cr and As ions from aqueous solutions. It was found that both ions were sorbed by the GGM-based hydrogels in considerable amounts. The sorption of Cr ions was highest at pH 3 and pH 9, whereas As ions sorbed more at pH 9 compared to acidic pH values. These changes in the sorption capacity at different pH values for As and Cr are arising from the changing nature of the metallic ions at different pH values. Overall it could be shown that tailor-made hydrogels with defined physical properties using derivatized GGM can be applied as biosorbents for the removal of toxic ions. These results will be the foundation for the development of GGM-MA containing biocomposites (e.g. together with nanofibrillated cellulose as a reinforcing matrix), which could be assessed as a column material for an efficient and environmentally friendly wastewater treatment.

Acknowledgements

Daniel Dax thanks the National Research Fund of Luxembourg (AFR) for granting him a scholarship (reference number 1000030). The Graduate School of Biomass Refining (BIOREGS) is thanked for financial support. Chunlin Xu thanks the funding from Knut and Alice Wallenberg Foundation via Wallenberg Wood Science Centre, Sweden. This work was also part of the activities at the Åbo Akademi Process Chemistry Centre. Julio Sánchez thanks FONDECYT (postdoctoral Grant No. 3120048) and CIPA, Chile.

Appendix A. Supplementary data

Supplementary data associated with this article can be found, in the online version, at http://dx.doi.org/10.1016/j.carbpol.2014.05.045.

References

Ahluwalia, S. S., & Goyal, D. (2005). Removal of heavy metals by waste tea leaves from aqueous solution. *Engineering in Life Sciences*, *5*(2), 158–162.
Akama, Y., & Ueda, T. (2013). Solid -phase extraction of Pb from common salt and water samples by cellulose modified with anhydrous EDTA. *Cellulose Chemistry Technology*, *47*(5–6), 479–486.
Al Manasrah, M., Kallioinen, M., Ilvesniemi, H., & Manttari, M. (2012). Recovery of galactoglucomannan from wood hydrolysate using regenerated cellulose ultrafiltration membranes. *Bioresource Technology*, *114*, 375–381.
Albertsson, A.-C., Voepel, J., Edlund, U., Dahlman, O., & Söderqvist-Lindblad, M. (2010). Design of renewable hydrogel release systems from fiberboard mill wastewater. *Biomacromolecules*, *11*(1406–1411), 1406.
Ali, I. O., Thabet, M. S., El-Nasser, K. S., Hassan, A. M., & Salama, T. M. (2012). Synthesis of nanosized ZSM-5 zeolite from rice straw using lignin as a template: Surface-modified zeolite with quaternary ammonium cation for removal of chromium from aqueous solution. *Microporous and Mesoporous Materials*, *160*, 97–105.
Apopei, D. F., Dinu, M. V., Trochimczuk, A. W., & Dragan, E. S. (2012). Sorption isotherms of heavy metal ions onto semi-interpenetrating polymer network cryogels based on polyacrylamide and anionically modified potato starch. *Industrial & Engineering Chemistry Research*, *51*(31), 10462–10471.
Ayoub, A., Venditti, R. A., Pawlak, J. J., Salam, A., & Hubbe, M. A. (2013). Novel hemicellulose–chitosan biosorbent for water desalination and heavy metal removal. *ACS Sustainable Chemistry & Engineering*, *1*(9), 1102–1109.
Dax, D., Eklund, P., Hemming, J., Sarfraz, J., Backman, P., Xu, C., et al. (2013). Amphiphilic spruce galactoglucomannan derivatives based on naturally-occurring fatty acids. *Bioresources*, *8*(3), 3771–3790.
Dax, D., Xu, C., Långvik, O., Hemming, J., Backman, P., & Willför, S. (2013). Synthesis of SET-LRP-induced galactoglucomannan-diblock copolymers. *Journal of Polymer Science Part A: Polymer Chemistry*, *51*(23), 5100–5110.
Faulconer, E. K., von Reitzenstein, N. V., & Mazyck, D. W. (2012). Optimization of magnetic powdered activated carbon for aqueous Hg(II) removal and magnetic recovery. *Journal of Hazardous Materials*, *199–200*, 9–14.
Feng, D., Aldrich, C., & Tan, H. (2000). Treatment of acid mine water by use of heavy metal precipitation and ion exchange. *Minerals Engineering*, *13*(6), 623–642.
Guo, X., Zhang, S., & Shan, X. Q. (2008). Adsorption of metal ions on lignin. *Journal of Hazardous Materials*, *151*(1), 134–142.
Hannuksela, T., & Hervé du Penhoat, C. (2004). NMR structural determination of dissolved O-acetylated galactoglucomannan isolated from spruce thermomechanical pulp. *Carbohydrate Research*, *339*(2), 301–312.
Kilpeläinen, P., Kitunen, V., Pranovich, A., Ivesmiemi, I., & Willför, S. (2013). Pressurized hot water flow-through extraction of birch sawdust with acetate pH buffer. *Bioresources*, *8*(4), 5202–5218.
Lundqvist, J., Jacobs, A., Palm, M., Zacchi, G., Dahlman, O., & Stålbrand, H. (2003). Characterization of galactoglucomannan extracted from spruce (*Picea abies*) by heat-fractionation at different conditions. *Carbohydrate Polymers*, *51*, 203–211.
Michielsen, S., Brandrup, J., & Immergut, E. H. (1999). *Polymer handbook*. New York: Wiley.
Netzahuatl-Muñoz, A., Guillén-Jiménez, F., Chávez-Gómez, B., Villegas-Garrido, T., & Cristiani-Urbina, E. (2012). Kinetic study of the effect of pH on hexavalent and trivalent chromium removal from aqueous solution by *Cupressus lusitanica* bark. *Water, Air, & Soil Pollution*, *223*(2), 625–641.
Palma, G., Freer, J., & Baeza, J. (2003). Removal of metal ions by modified *Pinus radiata* bark and tannins from water solutions. *Water Research*, *37*(20), 4974–4980.
Peng, X., Ren, J., Zhong, L., Sun, R., Shi, W., & Hu, B. (2012). Glycidyl methacrylate derivatized xylan-rich hemicelluloses: Synthesis and characterizations. *Cellulose*, *19*(4), 1361–1372.
Peng, X. W., Zhong, L. X., Ren, J. L., & Sun, R. C. (2012). Highly effective adsorption of heavy metal ions from aqueous solutions by macroporous xylan-rich

hemicelluloses-based hydrogel. *Journal of Agricultural and Food Chemistry*, *60*(15), 3909–3916.
Persson, T., Nordin, A.-K., Zacchi, G., & Jónsson, A.-S. (2007). Economic evaluation of isolation of hemicelluloses from process streams from thermomechanical pulping of spruce. *Applied Biochemistry and Biotechnology*, *136–140*, 741–752.
Rivas, B. L., & Muñoz, C. (2009). Functional water-insoluble polymers with ability to remove arsenic(V). *Polymer Bulletin*, *65*(1), 1–11.
Rivas, B. L., Pereira, E. D., Gallegos, P., & Geckeler, K. E. (2002). Water-soluble acidic polyelectrolytes with metal-removing ability. *Polymers for Advanced Technologies*, *13*(10–12), 1000–1005.
Rivas, B. L., Pereira, E. D., Palencia, M., & Sánchez, J. (2011). Water-soluble functional polymers in conjunction with membranes to remove pollutant ions from aqueous solutions. *Progress in Polymer Science*, *36*(2), 294–322.
Sánchez, J., Bastrzyk, A., Rivas, B. L., Bryjak, M., & Kabay, N. (2013). Removal of As(V) using liquid-phase polymer-based retention (LPR) technique with regenerated cellulose membrane as a filter. *Polymer Bulletin*, *70*(9), 2633–2644.
Voepel, J., Edlund, U., Albertsson, A.-C., & Percec, V. (2011). Hemicellulose-based multifunctional macroinitiator for single-electron-transfer mediated living radical polymerization. *Biomacromolecules*, *12*, 253–259.
Wan Ngah, W. S., & Hanafiah, M. A. (2008). Removal of heavy metal ions from wastewater by chemically modified plant wastes as adsorbents: A review. *Bioresource Technology*, *99*(10), 3935–3948.
Willför, S., Sjöholm, R., Laine, C., Roslund, M., Hemming, J., & Holmbom, B. (2003). Characterisation of water-soluble galactoglucomannans from Norway spruce wood and thermomechanical pulp. *Carbohydrate Polymers*, *52*, 175–187.
Willför, S., Sundberg, K., Tenkanen, M., & Holmbom, B. (2008). Spruce-derived mannans – A potential raw material for hydrocolloids and novel advanced natural materials. *Carbohydrate Polymers*, *72*(2), 197–210.
Xu, C., Leppänen, A.-S., Eklund, P., Holmlund, P., Sjöholm, R., Sundberg, K., et al. (2010). Acetylation and characterization of spruce (*Picea abies*) galactoglucomannans. *Carbohydrate Research*, *345*(6), 810–816.
Xu, C., Willför, S., Holmlund, P., & Holmbom, B. (2009). Rheological properties of water-soluble spruce O-acetyl galactoglucomannans. *Carbohydrate Polymers*, *75*(3), 498–504.
Zainol, Z., & Nicol, M. J. (2009). Comparative study of chelating ion exchange resins for the recovery of nickel and cobalt from laterite leach tailings. *Hydrometallurgy*, *96*(4), 283–287.
Zheng, Y., Wang, W., Zhu, G., & Wang, A. (2013). Enhanced selectivity for heavy metals using polyaniline-modified hydrogel. *Industrial & Engineering Chemistry Research*, *52*(13), 4957–4961.